Steel and Composite Structures, *Vol. 21, No. 6 (2016) 1227-1250*
DOI: http://dx.doi.org/10.12989/scs.2016.21.6.1227

Investigation on SCFs of concrete-filled circular chord and square braces K-joints under balanced axial loading

Yu Chen*, Kang Hu and Jian Yang

School of Urban Construction, Yangtze University, Jingzhou, China

(*Received March 03, 2016, Revised July 28, 2016, Accepted August 03, 2016*)

Abstract. Most of the research work has been conducted on K-joints under static loading. Very limited information is available in consideration of fatigue strength of K-joints with concrete-filled chord. This paper aims to describe experimental and numerical investigations on stress concentration factors (SCFs) of concrete-filled circular chord and square braces K-joints under balanced axial loading. Experiment was conducted to study the hot spot stress distribution along the intersection of chord and braces in the two specimens with compacting concrete filled in the chord. The test results of stress distribution curves of two specimens were reported. SCFs of concrete-filled circular chord and square braces K-joints were lower than those of corresponding hollow circular chord and square brace K-joints. The corresponding finite element analysis was also conducted to simulate stress distribution along the brace and chord intersection region of joints. It was achieved that experimental and finite element analysis results had good agreement. Therefore, an extensive parametric study was carried out by using the calibrated finite element model to evaluate the effects of main geometric parameters and concrete strength on the behavior of concrete-filled circular chord and square braces K-joints under balanced axial loading. The SCFs at the hot spot locations obtained from ABAQUS were compared with those calculated by using design formula given in the CIDECT for hollow SHS-SHS K-joints. CIDECT Design Guide was generally quite conservative for predicting SCFs of braces and was dangerous for predicting SCFs of chord in concrete-filled circular chord and square braces K-joints. Finally SCF formulae were proposed for circular chord and square braces K-joints with concrete-filled in the chord under balanced axial loading. It is shown that the SCFs calculated from the proposed design equation are generally in agreement with the values derived from finite element analysis, which were proved to be reliable and accurate.

Keywords: experimental investigation; finite element analysis; parametric study; stress concentration factor; concrete-filled chord; circular chord and square braces K-joints

1. Introduction

Welded tubular joints made of circular hollow sections (CHS) and square hollow sections (SHS) have been widely used in civil engineering due to their fast construction, light weight, aesthetic appearance and high strength. So, it has important significance to study fatigue property of circular hollow sections (CHS) and square hollow sections (SHS) joints under fatigue loading in practical space engineering.

Many researchers have been conducted in recent years on SCF formulae for different configurations of tubular joints under various types of basic loading. Cracked tubular K-joints

*Corresponding author, Professor, E-mail: kinkingingin@163.com

 ISSN: 1229-9367 (Print), 1598-6233 (Online)

were numerically investigated by Shao (2006). A new mesh generator for a tubular K-joint with a surface crack was developed and finite element analysis of stress intensity factor for cracked K-joint was conducted by using the proposed numerical modelling. Stress distribution in the vicinity of the weld fillet for notched welded tubular T-joints was investigated by Diaye *et al*. (2007). Parametric equations to predict stress concentration factor (SCF) of completely overlapped tubular joints under lap brace in-plane bending (IPB) load were proposed by Gao *et al*. (2007). Stress intensity factor rose as the radius increases at the notch bottom. Stress concentration factors of four full-size dragline tubular joints were experimentally investigated by Pang *et al*. (2009). Lee *et al*. (2009a, b) conducted fatigue study of partially overlapped circular hollow section K-joints and gave the validation of the numerical results. Experimental and numerical investigations on stress concentration factors of cold formed stainless steel square and rectangular hollow section X-joints were experimentally and numerically investigated by Feng and Young (2013). A unified design equation for the SCFs of cold-formed stainless steel tubular X-joints was proposed. Ahmadi *et al*. [8-9] investigated geometrically parametric effects of chord-side SCF distribution of central brace on internally ring-stiffened tubular KT-joints. Ahmadi *et al*. (2013) experimentally investigated KT-joints under three different axial loading conditions, in which a new propose of SCF design equations was established for fatigue design of three-planar KT-joints under three different axial loading cases. Ahmadi *et al*. (Ahmadi *et al*. 2011, Ahmadi and Lotfollahi-Yaghin 2013) attempted to study the stress concentration factor of DKT-joints in offshore jacket structures by using numerical analysis approach. Cao *et al*. (2013) conducted finite element analysis to estimate the ultimate load capacities of K-joints under axial loading. Numerical study on stress concentration square bird-beak square hollow section (SHS) welded joints were conducted by Cheng *et al*. (2015). Stress concentration factors of negative large eccentricity tubular N-joints under axial compressive loading in vertical brace were experimentally and numerically investigated by Yang and Chen (2015). Design formulae of stress concentration factors are available in CIDECT Design Guide No. 8 (Zhao *et al*. 2001) for SHS and CHS K-joints under balanced axial loading.

However, few researches have been carried out on stress concentration factors of concrete-filled steel tubular joints. The research on the concrete-filled CHS-SHS K-joints is concluded as follows. The fatigue behavior of CHS brace and concrete-filled CHS chord T-joints were investigated by Wang and Tong (2013). SCF distributions of hollow and concrete-filled CHS T-joints were compared. Tong *et al*. (2008) experimentally investigated concrete-filled CHS K-joints and welded CHS K-joints under axial loading, in which the SCFs at the concrete-filled CHS K-joints tended to be more significantly conservative compared with CHS K-joints. Chen *et al*. (2010) experimentally investigated concrete-filled CHS T-joints and welded CHS T-joints under in-plane bending and axial loading, in which the SCFs for T-joints at each loading conditions tended to be more uniform and significantly smaller compared with resent design codes. Hysteresis of concrete-filled circular tubular T-joints under axial load was experimentally and numerically investigated by Liu *et al*. (2015).

There is a lack of research carried out on the fatigue behavior of concrete-filled circular chord and square braces K-joints under balanced axial loading. Therefore, the stress concentration factors of concrete-filled circular chord and square braces K-joints under axial load need further investigation. In this paper, the experimental work was conducted on concrete-filled circular chord and square braces K-joints under balanced axial loading, the effect of concrete filled in chord on SCFs of joints under balanced axial loading were investigated. Furthermore, finite element analysis was also performed to evaluate the effects of several important geometric parameters, i.e. β (ratio of brace side length to chord diameter), 2γ (ratio of chord diameter to chord thickness), τ

(ratio of brace thickness to chord thickness) and φ (strength grade of concrete) on SCFs of concrete-filled circular chord and square braces K-joints. The design equations of SCFs are also proposed for concrete-filled circular chord and square braces K-joints under balanced axial loading.

2. Experimental investigation

2.1 Test specimen

Fig. 1 shows the dimensions and parameter definitions of hollow and concrete-filled circular chord and square braces K-joints specimen. The test specimens were fabricated from the circular hollow section steel tube of chord and square hollow section steel tubes of brace. The chord of one specimen was fully filled with self-compact concrete along the full length. As specified in CIDECT Design Guide No. 8 (Zhao *et al*. 2001), the specimens of K-joints were designed with non eccentricity in the range of allowable error. The geometric size and numbers of the two full scale circular chord and square braces K-joints are shown in Table 1.

(a) Hollow section

(b) Concrete filled in chord

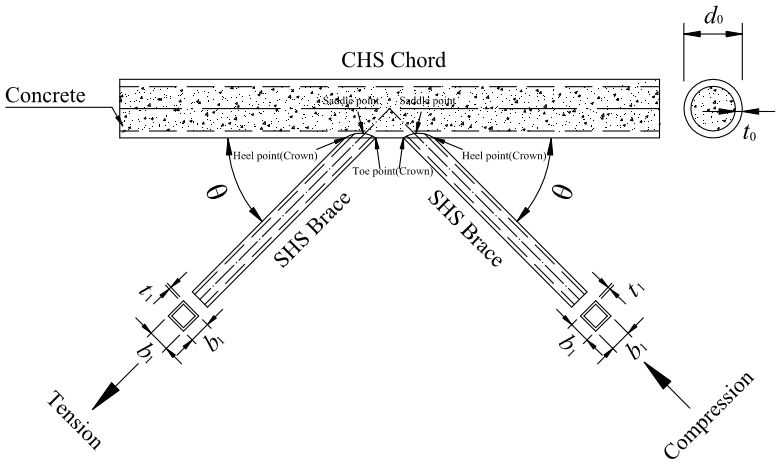

(c) Dimensions

Fig. 1 Circular chord and square braces K-joints specimens

Table 1 Details of test specimens

Specimen	Chord		Brace		β	2γ	τ	Concrete strength (Mpa)
	Diameter d_0 (mm)	Thickness t_0 (mm)	Diameter d_1 (mm)	Thickness t_1 (mm)				
K-108-4.5	108	4.5	40	2	0.37	24	0.444	0
K-108-4.5C	108	4.5	40	2	0.37	24	0.444	15

Two circular chord and square braces K-joints were manufactured for testing, which were made up of low carbon steel grade Q235B, in accordance with GB/T700-2006 (Chinese Standard 2006). Grade Q235B steel has a minimum specified yield stress of 235 MPa. Full penetration welds were adopted in all test specimens with gas metal arc welding method, in accordance with JGJ81-2002 (Chinese Standard 2002). Compressive cube strength of concrete in chord was designed as approximately 15 MPa. The compressive strength (f_{cu}) and elastic modulus (E_c) obtained from 150×150×150 (mm×mm×mm) cubes coupon test after 28 days' concrete curing were 11.6 MPa and 21,000 MPa, respectively.

In the process of fabricating joints, the strength grade of concrete filled in the chord is C15. Grade 32.5 Portland cement should be used in concrete mix proportion, and a small amount of fly ash should be added to improve the mechanical performance of the cement. Based on a great deal of test data, water cement ratio should be controlled at about 0.6. A cubic meter of concrete was made up of 300 kg of cement, 185 kg of water, 1165 kg of grave and 730 kg of sand.

In terms of their geometric type of joints, outer diameter of chord, and thickness of chord wall the specimens could be identified from the labelling. For example, the labels "K-108-4.5" and "K-108-4.5C" define the specimens as follow:

- The first letter indicates the type of the joint configuration, where the prefix "K" refers to K-joints.
- The following three digits indicate the nominal outer diameter of the chord of specimen in mm.
- The following one digit is the nominal thickness of chord wall in mm.
- The last letter "C" refers to the chord member fully filled with concrete. If there is no "C", it denotes hollow joints.

2.2 Test setup and loading scheme

A test setup was used to test these tubular K-joints under balanced axial loading, as shown in Fig. 2. Each specimen was pinned supported at the end of the braces. Axial compression force was applied to the bottom end plate of the chord member for K-joints to attain balanced axial loading in two braces. The length of chord for all joints were made longer than five chord diameters to make sure that the stresses at brace and chord intersections are not affected by the end condition.

Load control was used to drive the hydraulic actuator at a constant speed of 5 kN/min for all test specimens. The static stress concentration factors tests within elastic range were used to obtain the stresses (strains) along the brace and chord intersections. Strain gauges were also used to measure the strains of at the intersections in the test specimens. A data acquisition system (DH3816) was used to record the applied load and the readings of the strain gauges at regular intervals during the tests.

Fig. 2 Test setup of circular chord and square braces K-joints

(a) Overview

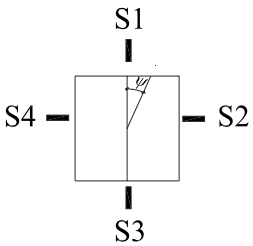

(c) Compressive brace

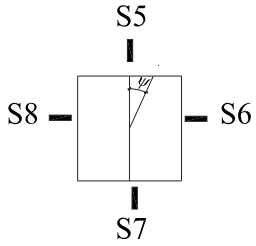

(d) Tensile brace

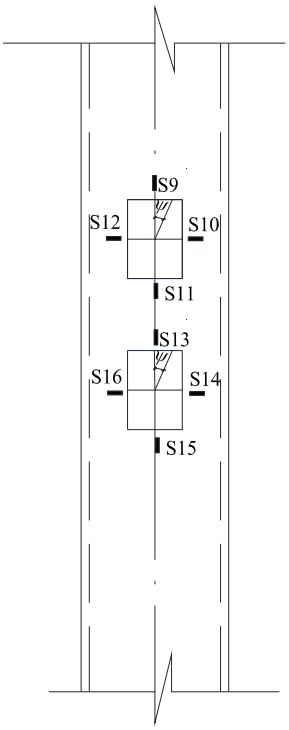

(b) Chord

Fig. 3 Strain gauges arrangement on circular chord and square braces K-joints

2.3 Strain gauge location

The position of the strain gauges and the extrapolation region were determined in line with the recommendation specified by CIDECT No. 8 (Zhao *et al*. 2001). Strain gauges S1-S4 were positioned at the root of compressive brace, Strain gauges S5-S8 were positioned at the root of

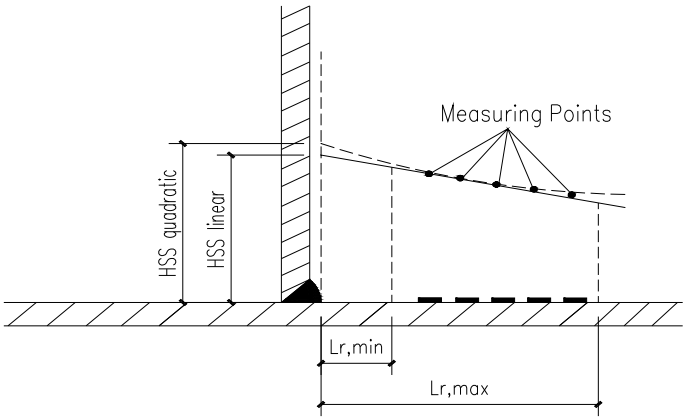

Fig. 4 Extrapolation methods of hot spot stress

tensile brace, and S9-S16 were positioned on the chord face, as illustrated in Fig. 3. ψ is defined as rotation degree of intersection line. Fig. 4 shows a schematic view of extrapolation methods of hotspot stress of concrete-filled circular chord and square braces K-joints. In Fig. 4 $L_{r,min}$ is the minimum length for extrapolation and $L_{r,max}$ is the maximum length for extrapolation.

The strain value of the two opposite surface are measured at mid-length of braces of concrete-filled circular chord and square braces K-joints under balanced axial loading to prove the braces are under the pure axial loading in tests. For instance, when the loading in chord of K-108-4.5C test specimen is 35kN, the opposite two axial strains in the mid-length of tensile brace is 47.95×10^{-6} and 48.50×10^{-6}, the opposite two axial strains in the mid-length of compressive brace is -52.13×10^{-6} and -49.39×10^{-6} by using strain gauges on brace surface. It can be secured that the braces are under the pure axial loads.

According to the boundary condition in experiments, it is cannot be secured that the braces are under the pure axial loads. It is better to prove it by strains measured at mid-length of braces. If not, please show the value of bending moment and its influence on the results.

2.4 Determination of SCF

In the fatigue behavior tests of circular chord and square braces K-joints, hot spot stress of circular chord and square braces K-joints could be measured by using gradient strain gauges. Because the geometrical size of strain gauge has its own requirements, so single strain gauge cannot be directly placed in welding seams area to measure the hot spot stress of the welding seams area. Usually gradient strain gauges were located in a specified interpolation area. According to CIDECT Design Guide No. 8 (Zhao *et al*. 2001), the interpolation area has a distance limitation from the welding seam. In the interpolation area five strain gauges were bonded around the welding seams. Thus the hot spot stress of the welding seams can be obtained from extrapolation stress in the interpolation area.

In the tests, the gradient strain gauges were located at 90 degree intervals around welding seams in two braces and chord interpolation area. At each saddle and crown point, due to the hot spot stress value might be different on brace and chord, so gradient strain gauges perpendicular to the welding seams were used to measure the SCFs of welding seams on brace and chord in the extrapolation. Based on measurement requirement of stress concentration factor in CIDECT

Design Guide No. 8 (Zhao *et al*. 2001), the shortest distance and the farthest distance from the welding seams of strain gauges on the chord were 10 mm and 18 mm, respectively. The shortest distance and the farthest distance from the welding seams of strain gauges on the brace were 8 mm and 10 mm, respectively. For concrete-filled circular chord and square braces K-joints, the quadratic extrapolation method was selected because of the strong non-linear strain distribution observed.

Stress concentration factor (SCF) is defined as the ratio of hot spot stress ($\sigma_{h.s}$) to nominal stress (σ_{nom}), i.e., SCF = $\sigma_{h.s}/\sigma_{nom}$. The nominal stress is determined by simple truss theory for joints under axial loading. Since SCF cannot be directly obtained in tests, strain concentration factor (SNCF) was measured and converted to SCF by means of relationship between SCF and SNCF, as in the previous research of welded tubular joints (Ahmadi *et al*. 2011). Similar to SCF, SNCF is defined as the ratio of geometrical hot spot strain (HSSN) to the nominal strain.

The HSSN $\xi_{\perp}$, which is perpendicular to the weld toe, and another strain component $\xi_{\parallel}$, which is parallel to the weld toe were obtained by using the quadratic extrapolation method based on the recommendation given in the CIDECT Design Guide for SHS and CHS tubular joints. The SNCF which is easier to obtain from strain gauge measurement can be calculated as

$$SNCF = \xi_{\perp} / \xi_n \tag{1}$$

Where ξ_n is the nominal strain obtained from single element strain gauges which were placed at the mid-length of brace or chord member. In order to obtain the SCF, the relationship between the SCF and SNCF needs to be determined. It was reported by Shao (2006) that the relationship between SCF and SNCF can be expressed as

$$SCF = \frac{1 + \upsilon \dfrac{\xi_{\parallel}}{\xi_{\perp}}}{1 - \upsilon^2} SNCF \tag{2}$$

where υ is Possion's ratio.

2.5 Experimental SCF distribution

Fig. 5 shows the SCF distribution of two specimens under axial loading. In terms of the hollow

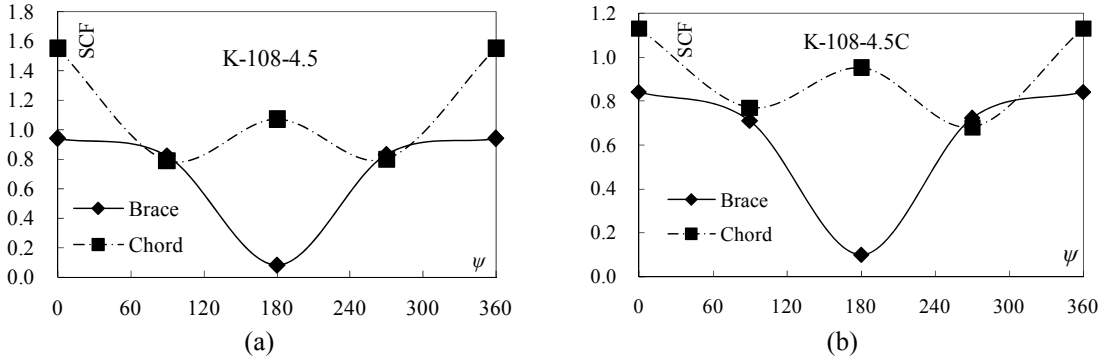

Fig. 5 SCF distribution in tests

section, for brace, the maximum stress concentration factor usually occurred at the heel point. Stress concentration factor reduced from the heel to toe point. For chord, the test results shown that the maximum stress concentration factor located at heel point, stress concentration factor decreased from the heel to saddle point gradually, and increased from saddle point to toe point gradually. For concrete-filled circular chord and square braces K-joints, the conclusion was similar to the hollow circular chord and square brace K-joints, but the SCFs of the concrete-filled circular chord and square braces K-joints were smaller than the SCFs of hollow circular chord and square brace K-joints.

3. Development and verification of finite element modeling

When finite element method was used to analyze the SCF distribution of hollow and concrete-filled circular chord and square braces K-joints, the precision of the numerical results obtained largely depends on the quality and quantity of finite element mesh. When finite element analysis was carried out on the joints, it should be concerned about the areas of high stress gradient, because the gradient stress was obvious in this intersection area. Therefore, in the area of high stress gradient, finite element mesh should be divided finely; in order to improve the computational efficiency, the low stress area could be meshed relatively coarse.

Based on the principles, the concrete-filled circular chord and square braces K-joints can be divided into different meshing area. Because of the hot spot stress in the welding seams, stress concentration factor is very high in the welding seams region, so the meshing of welding seams is fine. But the region far away from the welding seams, the stress concentration factor is small, these low stress areas can be used in coarse mesh in order to reduce computing time.

In order to verify the convergence of the finite element results, when tubes were divided into two layers in the direction of the thickness of tube, although computation time was short, but in the end the result accuracy was not high comparing with experimental results. When tubes along the wall thickness were divided into four layers, the result accuracy was high comparing with experimental results, but the computation time was too long. So tubes were divided into three layers in the direction of the thickness lastly, the high precision and effective time were obtained at the same time, as shown in Fig. 6(d). As a result, the welding seams were divided into six layers to obtain the effective computation results, as shown in Fig. 6(c).

Ratio of numerical SCF value to experimental SCF value is 1.15, 1.08, 1.04 and 1.02 respectively for K-108-4.5C test specimen FEA model with 35000, 40000, 45000 and 50000 element numbers. It is proved that the numerical results are stable with increase of elements when element number of joint FEA model is larger than 40000.

When ABAQUS was used to simulate joints, the damage criterion of concrete plasticity was adopted in the simulation of concrete in chord, the compressive and tensile properties of the constitutive relation was based on the different strength of the concrete which were acquired by coupon test. After a large number of finite element analysis, the concrete in chord was divided into ten layers to obtain the accurate computation results. Three-dimensional solid element C3D20R was used to model tubes, welding seam and concrete of concrete-filled circular chord and square braces K-joints, as shown in Fig. 6.

Fig. 7 shows the comparison of the SCFs determined from finite element models with experimental results for hollow and concrete-filled circular chord and square braces K-joints. The newly developed FE model for predicting SCFs of joints was verified to be accurate.

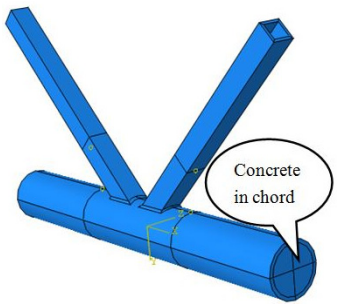

(a) Whole model

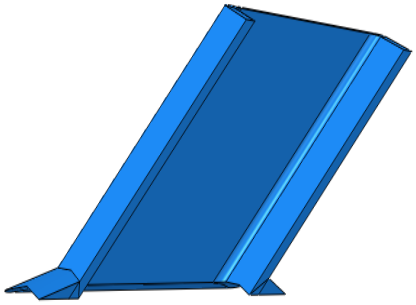

(b) Simulation of welding seam

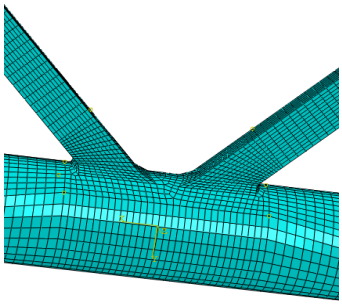

(c) Typical of mesh size

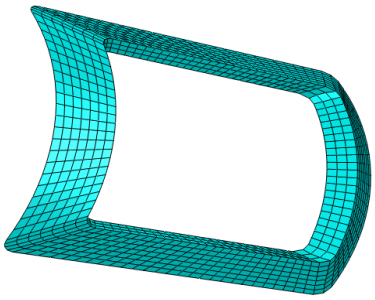

(d) Layers of welding seam element

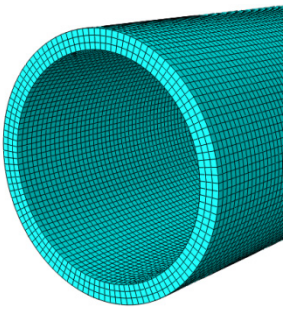

(e) Layers of CHS steel tubes

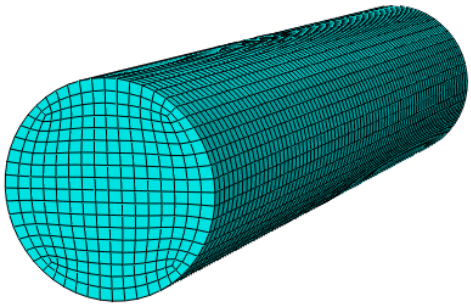

(f) Layers of concrete element

Fig. 6 FE mesh of circular chord and square braces K-joints

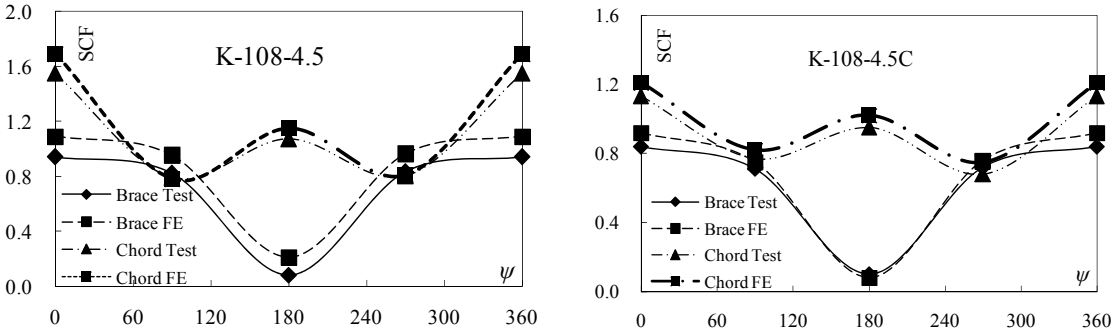

(a) (b)

Fig. 7 Comparison of SCF between FE analysis and test results

Table 2 Validity range of geometric parameters

Geometric parameters	$B = b_1/d_0$	$2\gamma = d_0/t_0$	$\tau = t_1/t_0$	φ
CIDECT (Zhao *et al*. 2001)	[0.35-1.00]	[10-35]	[0.25-1.00]	0
Eurocode 3 (2005)	[0.2-1.0]	[5-25]	-	0
Parametric study	[0.4-0.8]	[10-30]	[0.3-0.9]	[C30-C60]

4. Parametric study

4.1 Influential parameters

The stress concentration factors of concrete-filled circular chord and square braces K-joints is influenced by many factors, such as geometric parameters, loading type, boundary conditions, welding quality and initial defects. In this numerical study, effects of welding quality and the initial defects on SCFs were not considered. The ends of two braces were pinned connection. The angle value (θ) between two braces and chord is 45° in this symmetric structure. Stress concentration factor of concrete-filled circular chord and square braces K-joints under axial loading was determined by the geometrical parameters.

The effects of main geometric parameters on the SCFs of concrete-filled circular chord and square braces K-joints were separated, which include the β (ratio of brace side length to chord diameter), 2γ (ratio of chord diameter to chord thickness), τ (ratio of brace thickness to chord thickness), φ (strength grade of concrete). The validity range of these parametric variations in parametric study is summarized in the Table 2.

An extensive parametric study was carried out to evaluate the effects of main parametric variations on the SCFs of concrete-filled circular chord and square braces K-joints by using the verified finite element model. A total of 256 concrete-filled circular chord and square braces K-joints under balanced axial loading was analyzed in parametric study. The finite element specimens are labeled in terms of the non-dimensional parameters of K-joints. For example, the label "0.4-10-0.3-30" defined the K-joints with ratio of brace side length to chord diameter, ratio of chord diameter to chord thickness, ratio of brace thickness to chord thickness and strength grade of concrete in chord, respectively.

4.2 Numerical analysis

The influence of the parameters (β, 2γ, τ and φ) on SCFs of concrete-filled circular chord and square braces K-joints under axial loading caused by axial loading in the chord are illustrated in Fig. 8. SCF_{max} on chord of joints decreased as 2γ varied from 10 to 25 under axial loading, as shown in Fig. 8(k), l. SCF_{max} on chord of joints decreased as 2γ increased. As shown in Figs. 8(m), (n), SCF_{max} on chord increased as τ varied from 0.30 to 0.75. It can also be conclude that there was a positive correlation between SCF_{max} on chord of joints and τ. Similarly, Figs. 8(i), (j) shown the influence of non-dimensional parameter β on SCF_{max} was very complex. In other words, when β was less than 0.5, the maximum SCF was negative correlated with β; but the maximum SCF was positively correlated with β when the β was more than 0.5. The influence of φ on SCF_{max} was much smaller than the influence of 2γ, τ and β on SCF_{max}. As shown in Figs. 8(c), (d), (e), (f), (g), (h), the influence of non-dimensional parameter 2γ, τ and φ on SCF_{max} on brace was very small. As

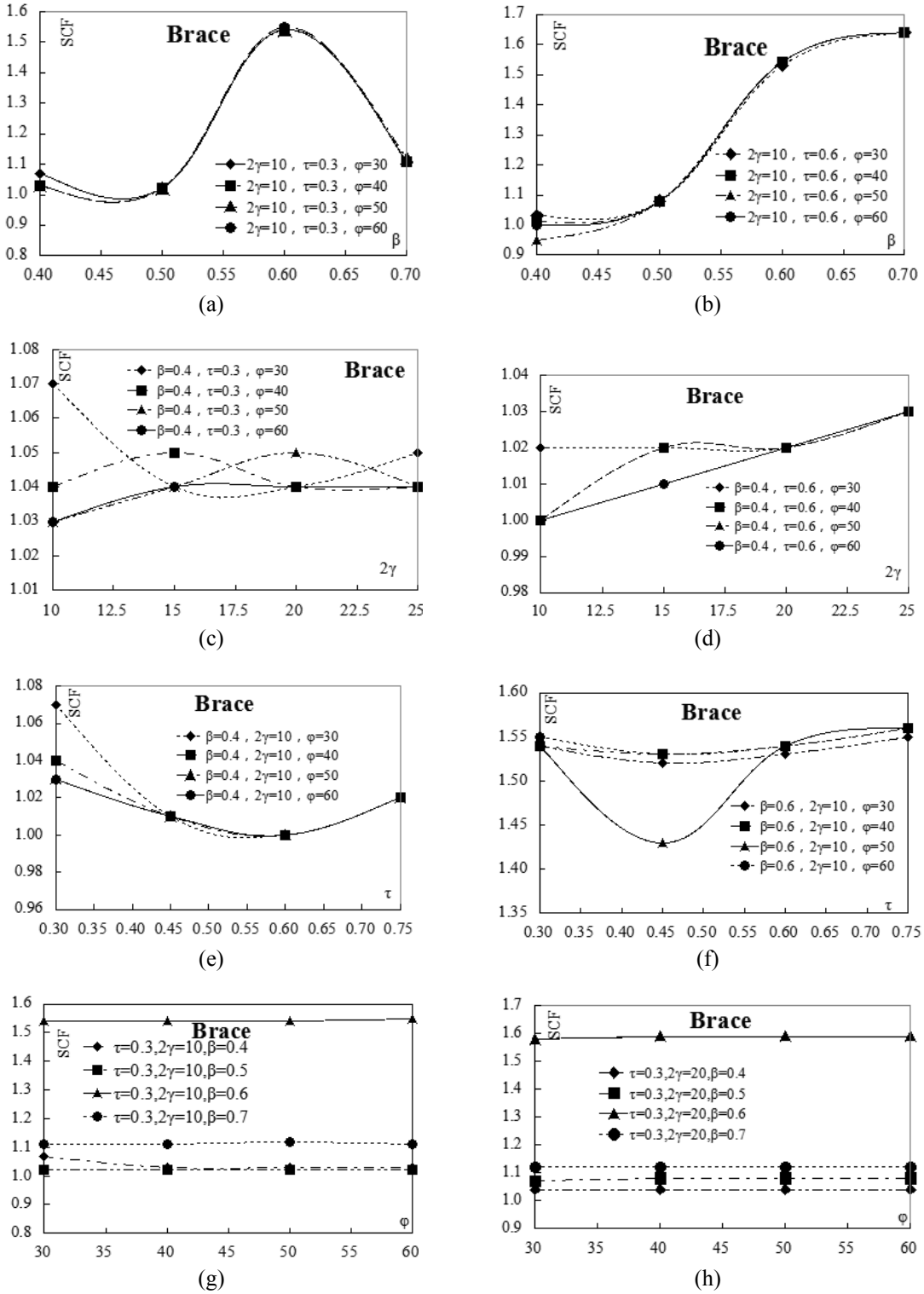

Fig. 8 Effect of β, 2γ , τ and φ on SCFs of joints

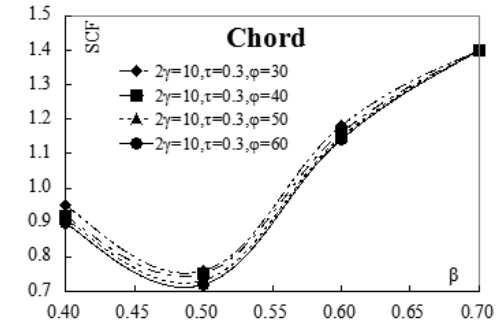

(i)

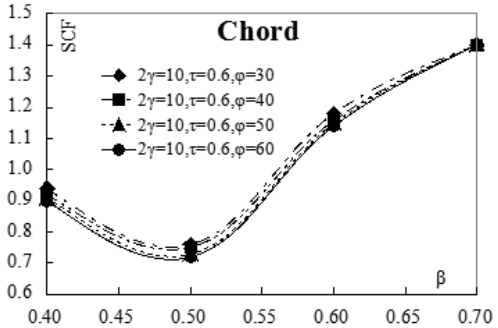

(j)

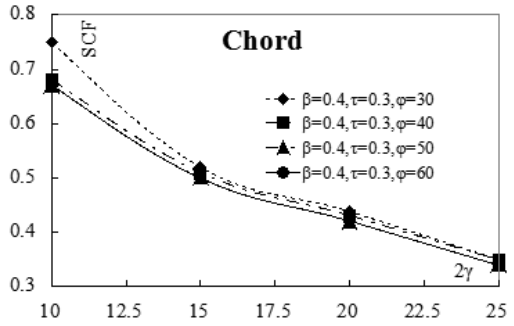

(k)

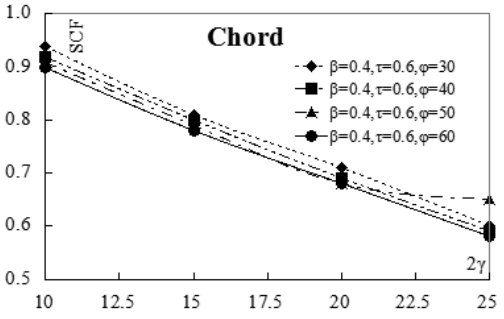

(l)

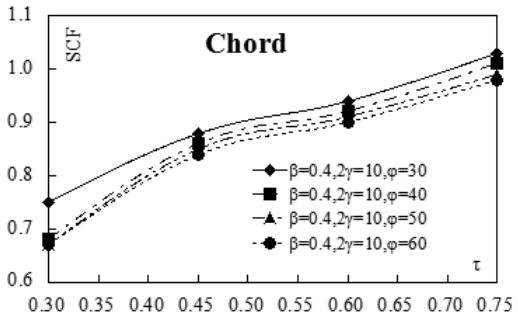

(m)

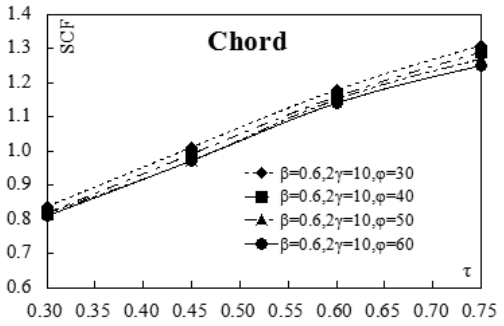

(n)

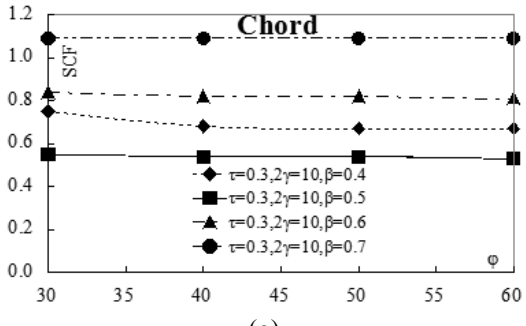

(o)

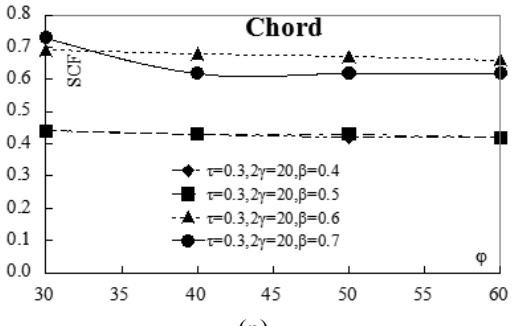

(p)

Fig. 8 Continued

shown in Figs. 8(a) and (b), the influence of non-dimensional parameter β on SCF_{max} for brace was very complex. In other words, the trend of the SCF_{max} for brace versus β was, to some extent, influenced by τ value.

The SCFs obtained from the parametric study were compared with the SCFs calculated using the design formula given in the CIDECT Design Guide No. 8 (Zhao *et al*. 2001). It should be noted that the design equations are only fit for SHS or CHS braces and chord joints. The SCFs of SHS-SHS K-joints under balanced axial loading can be determined using the following parametric equations given in the CIDECT Design Guide No. 8 (Zhao *et al*. 2001):

Chord member:.

$$SCF = (-0.572 \cdot \beta^2 - 0.022 \cdot \beta + 1.325) \cdot (2\gamma)^{0.455} \cdot (\tau)^{-0.969} \cdot (\sin(\theta))^{4.98} \tag{3}$$

Brace member:

$$SCF_{b,ax} = (-0.008 + 0.45 \cdot \beta - 0.34 \cdot \beta^2) \cdot (2\gamma)^{1.36} \cdot (\tau)^{-0.66} \cdot (\sin(\theta))^{1.29} \tag{4}$$

Although there are no corresponding equations for circular chord and square braces K-joints in CIDECT design guide, it is still really meaningful to compare the experimental data with similar relevant equations for square chord and braces K-joints. Comparisons were made between the SCF value obtained by finite element analysis results and those predicted by design methods, as shown in Table 3. From the Table 3, SCFs obtained from the finite element analysis are compared with the SCFs calculated using the CIDECT Design Guide equation for hollow SHS-SHS K-joints. A bad agreement was obtained with the mean value of FE SCF-to-CIDECT SCF ratio (SCF_{FE}/SCF_{CID}) for brace and chord of 0.87 and 1.22, and the corresponding COV of 0.025 and 0.028, respectively. It is shown from the comparison that the design rules for the SCFs specified in the CIDECT Design Guide were generally quite conservative for brace and dangerous for chord of concrete-filled circular chord and square braces K-joints, respectively.

Table 3 Comparison of SCFs in finite element analysis with SCFs calculated using proposed design equation and CIDECT design

Specimen number	Brace					Chord				
	SCF_{FE}	SCF_P	SCF_{CID}	SCF_{FE} /SCF_{CID}	SCF_{FE}/ SCF_P	SCF_{FE}	SCF_P	SCF_{CID}	SCF_{FE}/ SCF_{CID}	SCF_{FE}/ SCF_P
0.4-10-0.3-30	1.07	0.88	1.28	0.84	0.98	0.75	0.27	0.34	2.18	1.70
0.4-10-0.3-40	1.03	0.88	1.28	0.81	0.94	0.68	0.26	0.34	2.02	1.57
0.4-10-0.3-50	1.03	0.88	1.28	0.81	0.94	0.67	0.26	0.33	2.01	1.57
0.4-10-0.3-60	1.03	0.88	1.28	0.80	0.94	0.67	0.25	0.33	2.04	1.58
0.4-10-0.45-30	1.01	0.86	1.25	0.81	0.94	0.88	0.43	0.55	1.59	1.24
0.4-10-0.45-40	1.01	0.86	1.25	0.81	0.94	0.86	0.42	0.54	1.58	1.23
0.4-10-0.45-50	1.01	0.86	1.25	0.81	0.94	0.85	0.41	0.54	1.59	1.24
0.4-10-0.45-60	1.01	0.86	1.25	0.81	0.94	0.84	0.41	0.53	1.59	1.24
0.4-10-0.6-30	1.00	0.85	1.23	0.81	0.94	0.94	0.60	0.78	1.21	0.94
0.4-10-0.6-40	1.00	0.85	1.23	0.81	0.94	0.92	0.59	0.76	1.21	0.94

Table 3 Continued

Specimen number	Brace					Chord				
	SCF_{FE}	SCF_{P}	SCF_{CID}	SCF_{FE} /SCF_{CID}	SCF_{FE}/ SCF_{P}	SCF_{FE}	SCF_{P}	SCF_{CID}	SCF_{FE}/ SCF_{CID}	SCF_{FE}/ SCF_{P}
0.4-10-0.6-50	1.00	0.85	1.23	0.81	0.94	0.91	0.58	0.75	1.21	0.94
0.4-10-0.6-60	1.00	0.85	1.23	0.81	0.94	0.90	0.57	0.74	1.21	0.94
0.4-10-0.75-30	1.02	0.84	1.21	0.84	0.98	1.03	0.78	1.01	1.02	0.79
0.4-10-0.75-40	1.02	0.84	1.22	0.84	0.98	1.01	0.76	0.99	1.02	0.79
0.4-10-0.75-50	1.02	0.84	1.22	0.84	0.97	0.99	0.75	0.98	1.01	0.79
0.4-10-0.75-60	1.02	0.84	1.22	0.84	0.97	0.98	0.74	0.97	1.02	0.79
0.4-15-0.3-30	1.04	0.85	1.23	0.84	0.98	0.52	0.26	0.34	1.53	1.19
0.4-15-0.3-40	1.04	0.85	1.23	0.84	0.98	0.51	0.26	0.33	1.53	1.19
0.4-15-0.3-50	1.04	0.85	1.24	0.84	0.98	0.50	0.25	0.33	1.52	1.18
0.4-15-0.3-60	1.04	0.85	1.24	0.84	0.98	0.50	0.25	0.33	1.54	1.19
0.4-15-0.45-30	1.03	0.83	1.20	0.85	0.99	0.68	0.42	0.55	1.24	0.97
0.4-15-0.45-40	1.03	0.83	1.21	0.85	0.99	0.67	0.41	0.54	1.25	0.97
0.4-15-0.45-50	1.02	0.83	1.21	0.84	0.98	0.66	0.41	0.53	1.25	0.97
0.4-15-0.45-60	1.02	0.83	1.21	0.84	0.98	0.66	0.40	0.52	1.26	0.98
0.4-15-0.6-30	1.02	0.82	1.19	0.86	1.00	0.81	0.59	0.77	1.06	0.82
0.4-15-0.6-40	1.02	0.82	1.19	0.86	0.99	0.80	0.58	0.75	1.06	0.83
0.4-15-0.6-50	1.02	0.82	1.19	0.86	0.99	0.79	0.57	0.74	1.06	0.83
0.4-15-0.6-60	1.01	0.82	1.19	0.85	0.98	0.78	0.57	0.73	1.06	0.83
0.4-15-0.75-30	1.01	0.81	1.17	0.86	1.00	0.83	0.77	1.00	0.83	0.65
0.4-10-0.75-40	1.01	0.81	1.17	0.86	1.00	0.81	0.76	0.98	0.83	0.64
0.4-15-0.75-50	1.00	0.81	1.18	0.85	0.98	0.80	0.74	0.97	0.83	0.64
0.4-15-0.75-60	1.00	0.81	1.18	0.85	0.98	0.79	0.74	0.95	0.83	0.64
0.4-20-0.3-30	1.04	0.83	1.20	0.87	1.00	0.44	0.26	0.34	1.31	1.01
0.4-20-0.3-40	1.04	0.83	1.20	0.86	1.00	0.43	0.26	0.33	1.30	1.01
0.4-20-0.3-50	1.04	0.83	1.21	0.86	1.00	0.42	0.25	0.33	1.29	1.00
0.4-20-0.3-60	1.04	0.83	1.21	0.86	1.00	0.42	0.25	0.32	1.30	1.01
0.4-20-0.45-30	1.03	0.81	1.18	0.88	1.02	0.57	0.42	0.54	1.05	0.82
0.4-20-0.45-40	1.03	0.81	1.18	0.87	1.02	0.56	0.41	0.53	1.05	0.82
0.4-20-0.45-50	1.03	0.81	1.18	0.87	1.02	0.55	0.41	0.53	1.05	0.82
0.4-20-0.45-60	1.03	0.81	1.18	0.87	1.01	0.54	0.40	0.52	1.04	0.81
0.4-20-0.6-30	1.02	0.80	1.16	0.88	1.02	0.71	0.59	0.76	0.93	0.73
0.4-20-0.6-40	1.02	0.80	1.16	0.88	1.02	0.69	0.58	0.75	0.92	0.72
0.4-20-0.6-50	1.02	0.80	1.16	0.88	1.02	0.68	0.57	0.74	0.92	0.72
0.4-20-0.6-60	1.02	0.80	1.16	0.88	1.02	0.68	0.56	0.73	0.93	0.73
0.4-20-0.75-30	1.02	0.79	1.14	0.89	1.03	0.82	0.76	0.99	0.83	0.64
0.4-20-0.75-40	1.02	0.79	1.15	0.89	1.03	0.81	0.75	0.97	0.83	0.65
0.4-20-0.75-50	1.01	0.79	1.15	0.88	1.02	0.80	0.74	0.96	0.84	0.65

Table 3 Continued

Specimen number	Brace					Chord				
	SCF_{FE}	SCF_{P}	SCF_{CID}	SCF_{FE} /SCF_{CID}	SCF_{FE}/ SCF_{P}	SCF_{FE}	SCF_{P}	SCF_{CID}	SCF_{FE}/ SCF_{CID}	SCF_{FE}/ SCF_{P}
0.4-20-0.75-60	1.01	0.79	1.15	0.88	1.02	0.79	0.73	0.95	0.83	0.65
0.4-25-0.3-30	1.05	0.81	1.18	0.89	1.03	0.35	0.26	0.33	1.05	0.81
0.4-25-0.3-40	1.04	0.81	1.18	0.88	1.02	0.35	0.	0.33	1.06	0.83
0.4-25-0.3-50	1.04	0.82	1.18	0.88	1.02	0.34	0.	0.32	1.05	0.82
0.4-25-0.3-60	1.04	0.82	1.18	0.88	1.02	0.34	0.25	0.32	1.06	0.82
0.4-25-0.45-30	1.04	0.80	1.15	0.90	1.05	0.47	0.42	0.54	0.87	0.68
0.4-25-0.45-40	1.03	0.80	1.15	0.89	1.03	0.46	0.41	0.53	0.87	0.68
0.4-25-0.45-50	1.03	0.80	1.16	0.89	1.03	0.46	0.40	0.52	0.88	0.68
0.4-25-0.45-60	1.03	0.80	1.16	0.89	1.03	0.45	0.40	0.52	0.87	0.68
0.4-25-0.6-30	1.03	0.78	1.14	0.91	1.05	0.60	0.58	0.76	0.79	0.62
0.4-25-0.6-40	1.30	0.78	1.14	1.14	1.33	0.59	0.57	0.74	0.79	0.62
0.4-25-0.6-50	1.03	0.79	1.14	0.90	1.05	0.65	0.56	0.73	0.89	0.69
0.4-25-0.6-60	1.03	0.79	1.14	0.90	1.05	0.58	0.56	0.72	0.80	0.62
0.4-25-0.75-30	1.02	0.77	1.12	0.91	1.06	0.72	0.76	0.98	0.73	0.57
0.4-25-0.75-40	1.02	0.78	1.12	0.91	1.06	0.70	0.74	0.96	0.73	0.56
0.4-25-0.75-50	1.02	0.78	1.13	0.91	1.05	0.69	0.73	0.95	0.73	0.56
0.4-25-0.75-60	1.02	0.78	1.13	0.91	1.05	0.68	0.73	0.94	0.72	0.56
0.5-10-0.3-30	1.02	1.13	1.53	0.66	0.73	0.55	0.30	0.38	1.46	1.12
0.5-10-0.3-40	1.02	1.13	1.54	0.66	0.72	0.54	0.29	0.37	1.46	1.12
0.5-10-0.3-50	1.02	1.13	1.54	0.66	0.72	0.54	0.29	0.36	1.49	1.13
0.5-10-0.3-60	1.02	1.13	1.54	0.66	0.72	0.53	0.28	0.36	1.47	1.12
0.5-10-0.45-30	1.03	1.10	1.50	0.69	0.75	0.67	0.48	0.60	1.11	0.85
0.5-10-0.45-40	1.04	1.10	1.50	0.69	0.75	0.65	0.47	0.59	1.09	0.83
0.5-10-0.45-50	1.04	1.10	1.51	0.69	0.75	0.64	0.46	0.59	1.09	0.83
0.5-10-0.45-60	1.04	1.11	1.51	0.69	0.75	0.63	0.46	0.58	1.09	0.83
0.5-10-0.6-30	1.08	1.08	1.48	0.73	0.80	0.76	0.67	0.85	0.90	0.68
0.5-10-0.6-40	1.08	1.09	1.48	0.73	0.79	0.75	0.66	0.83	0.90	0.68
0.5-10-0.6-50	1.08	1.09	1.48	0.73	0.79	0.73	0.65	0.82	0.89	0.68
0.5-10-0.6-60	1.08	1.09	1.48	0.73	0.79	0.72	0.64	0.81	0.89	0.68
0.4-10-0.75-30	1.10	1.07	1.46	0.75	0.82	0.83	0.87	1.10	0.75	0.58
0.5-10-0.75-40	1.10	1.07	1.46	0.75	0.82	0.82	0.85	1.08	0.76	0.58
0.5-10-0.75-50	1.10	1.07	1.46	0.75	0.82	0.81	0.84	1.07	0.76	0.58
0.5-10-0.75-60	1.10	1.08	1.47	0.75	0.82	0.80	0.83	1.05	0.76	0.58
0.5-15-0.3-30	1.07	1.09	1.48	0.72	0.78	0.57	0.29	0.37	1.54	1.17
0.5-15-0.3-40	1.08	1.09	1.48	0.73	0.79	0.56	0.29	0.36	1.54	1.17
0.5-15-0.3-50	1.08	1.09	1.49	0.73	0.79	0.55	0.28	0.36	1.53	1.16
0.5-15-0.3-60	1.08	1.09	1.49	0.73	0.79	0.54	0.28	0.36	1.52	1.16

Table 3 Continued

Specimen number	Brace					Chord				
	SCF_{FE}	SCF_{P}	SCF_{CID}	SCF_{FE} /SCF_{CID}	SCF_{FE}/ SCF_{P}	SCF_{FE}	SCF_{P}	SCF_{CID}	SCF_{FE}/ SCF_{CID}	SCF_{FE}/ SCF_{P}
0.5-15-0.45-30	1.07	1.06	1.45	0.74	0.81	0.75	0.47	0.60	1.25	0.95
0.5-15-0.45-40	1.07	1.07	1.45	0.74	0.80	0.74	0.46	0.59	1.26	0.96
0.5-15-0.45-50	1.07	1.07	1.45	0.74	0.80	0.73	0.46	0.58	1.26	0.96
0.5-15-0.45-60	1.08	1.07	1.46	0.74	0.81	0.72	0.45	0.57	1.26	0.96
0.5-15-0.6-30	1.05	1.05	1.43	0.74	0.80	0.88	0.66	0.84	1.05	0.80
0.5-15-0.6-40	1.05	1.05	1.43	0.73	0.80	0.87	0.65	0.82	1.06	0.80
0.5-15-0.6-50	1.05	1.05	1.43	0.73	0.80	0.85	0.64	0.81	1.05	0.80
0.5-15-0.6-60	1.05	1.05	1.43	0.73	0.80	0.84	0.63	0.80	1.05	0.80
0.5-15-0.75-30	1.05	1.03	1.41	0.74	0.81	0.87	0.86	1.09	0.80	0.61
0.5-10-0.75-40	1.05	1.04	1.41	0.74	0.81	0.85	0.84	1.07	0.79	0.61
0.5-15-0.75-50	1.06	1.04	1.41	0.75	0.82	0.84	0.83	1.06	0.80	0.61
0.5-15-0.75-60	1.06	1.04	1.42	0.75	0.82	0.83	0.82	1.04	0.80	0.61
0.5-20-0.3-30	1.07	1.06	1.45	0.74	0.81	0.44	0.29	0.37	1.19	0.91
0.5-20-0.3-40	1.08	1.06	1.45	0.75	0.82	0.43	0.29	0.36	1.19	0.91
0.5-20-0.3-50	1.08	1.06	1.45	0.75	0.81	0.43	0.28	0.36	1.21	0.92
0.5-20-0.3-60	1.08	1.07	1.45	0.74	0.81	0.42	0.28	0.35	1.19	0.91
0.5-20-0.45-30	1.08	1.04	1.41	0.76	0.83	0.60	0.47	0.59	1.01	0.77
0.5-20-0.45-40	1.08	1.04	1.42	0.76	0.83	0.59	0.46	0.58	1.01	0.77
0.5-20-0.45-50	1.08	1.04	1.42	0.76	0.83	0.58	0.45	0.57	1.01	0.77
0.5-20-0.45-60	1.09	1.04	1.42	0.77	0.84	0.58	0.45	0.57	1.02	0.78
0.5-20-0.6-30	1.07	1.02	1.39	0.77	0.84	0.73	0.66	0.83	0.88	0.67
0.5-20-0.6-40	1.07	1.02	1.39	0.77	0.84	0.71	0.64	0.82	0.87	0.66
0.5-20-0.6-50	1.07	1.02	1.40	0.77	0.83	0.70	0.63	0.81	0.87	0.66
0.5-20-0.6-60	1.08	1.03	1.40	0.77	0.84	0.70	0.63	0.80	0.88	0.67
0.5-20-0.75-30	1.06	1.01	1.38	0.77	0.84	0.83	0.85	1.08	0.77	0.58
0.5-20-0.75-40	1.06	1.01	1.38	0.77	0.84	0.82	0.84	1.06	0.77	0.59
0.5-20-0.75-50	1.07	1.01	1.38	0.78	0.85	0.80	0.83	1.05	0.76	0.58
0.5-20-0.75-60	1.07	1.01	1.38	0.77	0.85	0.79	0.82	1.03	0.76	0.58
0.5-25-0.3-30	1.07	1.04	1.42	0.75	0.82	0.36	0.29	0.37	0.98	0.75
0.5-25-0.3-40	1.08	1.04	1.42	0.76	0.83	0.35	0.28	0.36	0.97	0.74
0.5-25-0.3-50	1.08	1.04	1.42	0.76	0.82	0.35	0.28	0.35	0.99	0.75
0.5-25-0.3-60	1.08	1.04	1.42	0.76	0.82	0.34	0.28	0.35	0.97	0.74
0.5-25-0.45-30	1.07	1.02	1.39	0.77	0.84	0.50	0.46	0.59	0.85	0.65
0.5-25-0.45-40	1.07	1.02	1.39	0.77	0.84	0.49	0.46	0.58	0.85	0.64
0.5-25-0.45-50	1.07	1.02	1.39	0.77	0.84	0.48	0.45	0.57	0.84	0.64
0.5-25-0.45-60	1.07	1.02	1.39	0.77	0.84	0.48	0.44	0.56	0.85	0.65
0.5-25-0.6-30	1.07	1.00	1.37	0.78	0.86	0.61	0.65	0.83	0.74	0.56

Table 3 Continued

Specimen number	Brace					Chord				
	SCF_{FE}	SCF_{P}	SCF_{CID}	SCF_{FE} /SCF_{CID}	SCF_{FE}/ SCF_{P}	SCF_{FE}	SCF_{P}	SCF_{CID}	SCF_{FE}/ SCF_{CID}	SCF_{FE}/ SCF_{P}
0.5-25-0.6-40	1.08	1.00	1.37	0.79	0.86	0.60	0.64	0.81	0.74	0.56
0.5-25-0.6-50	1.08	1.01	1.37	0.79	0.86	0.59	0.63	0.80	0.74	0.56
0.5-25-0.6-60	1.08	1.01	1.37	0.79	0.86	0.59	0.62	0.79	0.75	0.57
0.5-25-0.75-30	0.87	0.99	1.35	0.64	0.70	0.57	0.85	1.07	0.53	0.40
0.5-25-0.75-40	1.07	0.99	1.35	0.79	0.86	0.69	0.83	1.05	0.65	0.50
0.5-25-0.75-50	1.07	0.99	1.35	0.79	0.86	0.68	0.82	1.04	0.65	0.50
0.5-25-0.75-60	1.08	0.99	1.35	0.80	0.87	0.68	0.81	1.03	0.66	0.50
0.6-10-0.3-30	1.54	1.21	1.62	0.95	1.02	0.84	0.33	0.41	2.05	1.53
0.6-10-0.3-40	1.54	1.21	1.63	0.95	1.02	0.82	0.32	0.40	2.04	1.52
0.6-10-0.3-50	1.54	1.22	1.63	0.95	1.02	0.82	0.32	0.40	2.07	1.55
0.6-10-0.3-60	1.55	1.22	1.63	0.95	1.02	0.81	0.31	0.39	2.07	1.54
0.6-10-0.45-30	1.52	1.19	1.59	0.96	1.02	1.01	0.53	0.66	1.53	1.15
0.6-10-0.45-40	1.53	1.19	1.59	0.96	1.03	0.99	0.52	0.65	1.53	1.14
0.6-10-0.45-50	1.43	1.19	1.59	0.90	0.96	0.97	0.51	0.64	1.52	1.13
0.6-10-0.45-60	1.53	1.19	1.60	0.96	1.03	0.97	0.51	0.63	1.54	1.15
0.6-10-0.6-30	1.53	1.17	1.56	0.98	1.05	1.18	0.74	0.92	1.28	0.95
0.6-10-0.6-40	1.54	1.17	1.57	0.98	1.06	1.16	0.73	0.91	1.28	0.95
0.6-10-0.6-50	1.54	1.17	1.57	0.98	1.06	1.15	0.72	0.89	1.28	0.96
0.6-10-0.6-60	1.54	1.17	1.57	0.98	1.05	1.14	0.71	0.88	1.29	0.96
0.6-10-0.75-30	1.55	1.15	1.55	1.00	1.07	1.31	0.96	1.20	1.09	0.82
0.6-10-0.75-40	1.56	1.16	1.55	1.01	1.08	1.29	0.95	1.18	1.09	0.82
0.6-10-0.75-50	1.56	1.16	1.55	1.01	1.08	1.27	0.93	1.16	1.09	0.82
0.6-10-0.75-60	1.56	1.16	1.55	1.01	1.08	1.25	0.92	1.15	1.09	0.81
0.6-15-0.3-30	1.58	1.17	1.57	1.01	1.08	0.89	0.33	0.40	2.20	1.64
0.6-15-0.3-40	1.58	1.17	1.57	1.01	1.08	0.87	0.32	0.40	2.19	1.64
0.6-15-0.3-50	1.58	1.17	1.57	1.00	1.08	0.86	0.31	0.39	2.19	1.64
0.6-15-0.3-60	1.59	1.17	1.57	1.01	1.08	0.85	0.31	0.39	2.19	1.64
0.6-15-0.45-30	1.56	1.14	1.53	1.02	1.09	1.18	0.52	0.65	1.81	1.35
0.6-15-0.45-40	1.56	1.15	1.54	1.01	1.09	1.17	0.51	0.64	1.83	1.37
0.6-15-0.45-50	1.57	1.15	1.54	1.02	1.10	1.15	0.51	0.63	1.82	1.36
0.6-15-0.45-60	1.57	1.15	1.54	1.02	1.10	1.14	0.50	0.62	1.83	1.36
0.6-15-0.6-30	1.54	1.13	1.51	1.02	1.10	1.42	0.73	0.91	1.55	1.16
0.6-15-0.6-40	1.55	1.13	1.51	1.02	1.10	1.39	0.72	0.90	1.55	1.16
0.6-15-0.6-50	1.55	1.13	1.52	1.02	1.10	1.37	0.71	0.88	1.55	1.16
0.6-15-0.6-60	1.56	1.13	1.52	1.03	1.10	1.36	0.70	0.87	1.55	1.16
0.6-15-0.75-30	1.51	1.11	1.49	1.01	1.09	1.37	0.95	1.19	1.15	0.86
0.6-10-0.75-40	1.52	1.12	1.50	1.02	1.09	1.34	0.94	1.17	1.15	0.86

Table 3 Continued

Specimen number	Brace					Chord				
	SCF_{FE}	SCF_{P}	SCF_{CID}	SCF_{FE} /SCF_{CID}	SCF_{FE}/ SCF_{P}	SCF_{FE}	SCF_{P}	SCF_{CID}	SCF_{FE}/ SCF_{CID}	SCF_{FE}/ SCF_{P}
0.6-15-0.75-50	1.52	1.12	1.50	1.02	1.09	1.33	0.92	1.15	1.16	0.86
0.6-15-0.75-60	1.52	1.12	1.50	1.01	1.09	1.31	0.91	1.14	1.15	0.86
0.6-20-0.3-30	1.58	1.14	1.53	1.03	1.10	0.69	0.32	0.40	1.72	1.28
0.6-20-0.3-40	1.59	1.14	1.53	1.04	1.11	0.68	0.32	0.39	1.72	1.29
0.6-20-0.3-50	1.59	1.14	1.53	1.04	1.11	0.67	0.31	0.39	1.72	1.29
0.6-20-0.3-60	1.59	1.15	1.54	1.03	1.11	0.66	0.31	0.38	1.72	1.28
0.6-20-0.45-30	1.57	1.12	1.50	1.05	1.13	0.96	0.52	0.65	1.48	1.11
0.6-20-0.45-40	1.57	1.12	1.50	1.05	1.12	0.94	0.51	0.63	1.48	1.10
0.6-20-0.45-50	1.58	1.12	1.50	1.05	1.13	0.93	0.50	0.63	1.49	1.11
0.6-20-0.45-60	1.58	1.12	1.50	1.05	1.13	0.92	0.50	0.62	1.49	1.11
0.6-20-0.6-30	1.56	1.10	1.47	1.06	1.14	1.17	0.73	0.91	1.29	0.97
0.6-20-0.6-40	1.56	1.10	1.48	1.06	1.14	1.15	0.72	0.89	1.29	0.97
0.6-20-0.6-50	1.57	1.10	1.48	1.06	1.14	1.14	0.71	0.88	1.30	0.97
0.6-20-0.6-60	1.57	1.10	1.48	1.06	1.14	1.12	0.70	0.87	1.29	0.97
0.6-20-0.75-30	1.54	1.09	1.46	1.06	1.14	1.34	0.95	1.18	1.14	0.85
0.6-20-0.75-40	1.55	1.09	1.46	1.06	1.14	1.32	0.93	1.16	1.14	0.85
0.6-20-0.75-50	1.55	1.09	1.46	1.06	1.14	1.30	0.92	1.14	1.14	0.85
0.6-20-0.75-60	1.56	1.09	1.46	1.07	1.14	1.29	0.91	1.13	1.14	0.85
0.6-25-0.3-30	1.58	1.12	1.50	1.05	1.13	0.58	0.32	0.40	1.45	1.09
0.6-25-0.3-40	1.58	1.12	1.50	1.05	1.13	0.57	0.31	0.39	1.45	1.09
0.6-25-0.3-50	1.58	1.12	1.51	1.05	1.13	0.56	0.31	0.39	1.45	1.08
0.6-25-0.3-60	1.59	1.12	1.51	1.05	1.13	0.55	0.31	0.38	1.44	1.07
0.6-25-0.45-30	1.58	1.10	1.47	1.08	1.15	0.80	0.52	0.64	1.25	0.93
0.6-25-0.45-40	1.58	1.10	1.47	1.07	1.15	0.78	0.51	0.63	1.24	0.92
0.6-25-0.45-50	1.59	1.10	1.47	1.08	1.16	0.77	0.50	0.62	1.24	0.92
0.6-25-0.45-60	1.59	1.10	1.47	1.08	1.16	0.76	0.49	0.62	1.24	0.92
0.6-25-0.6-30	1.57	1.08	1.45	1.09	1.17	0.93	0.72	0.90	1.03	0.77
0.6-25-0.6-40	1.58	1.08	1.45	1.09	1.17	0.98	0.71	0.88	1.11	0.83
0.6-25-0.6-50	1.58	1.08	1.45	1.09	1.17	0.96	0.70	0.87	1.10	0.82
0.6-25-0.6-60	1.59	1.08	1.45	1.10	1.18	0.96	0.69	0.86	1.11	0.83
0.6-25-0.75-30	1.56	1.07	1.43	1.09	1.17	1.16	0.94	1.17	0.99	0.74
0.6-25-0.75-40	1.56	1.07	1.43	1.09	1.17	1.14	0.92	1.15	0.99	0.74
0.6-25-0.75-50	1.57	1.07	1.43	1.10	1.18	1.12	0.91	1.13	0.99	0.74
0.6-25-0.75-60	1.57	1.07	1.43	1.09	1.18	1.11	0.90	1.12	0.99	0.74
0.7-10-0.3-30	1.11	1.14	1.55	0.72	0.78	1.09	0.36	0.44	2.45	1.80
0.7-10-0.3-40	1.11	1.14	1.55	0.72	0.78	1.09	0.36	0.44	2.49	1.83
0.7-10-0.3-50	1.12	1.14	1.55	0.72	0.78	1.09	0.35	0.43	2.53	1.86

Table 3 Continued

Specimen number	Brace					Chord				
	SCF_{FE}	SCF_{P}	SCF_{CID}	SCF_{FE} /SCF_{CID}	SCF_{FE}/ SCF_{P}	SCF_{FE}	SCF_{P}	SCF_{CID}	SCF_{FE}/ SCF_{CID}	SCF_{FE}/ SCF_{P}
0.7-10-0.3-60	1.11	1.14	1.55	0.72	0.78	1.09	0.35	0.43	2.56	1.88
0.7-10-0.45-30	1.32	1.11	1.51	0.87	0.95	1.44	0.59	0.72	2.01	1.48
0.7-10-0.45-40	1.32	1.11	1.51	0.87	0.94	1.44	0.57	0.70	2.05	1.51
0.7-10-0.45-50	1.32	1.12	1.52	0.87	0.94	1.44	0.57	0.69	2.08	1.52
0.7-10-0.45-60	1.32	1.12	1.52	0.87	0.94	1.44	0.56	0.69	2.10	1.54
0.7-10-0.6-30	1.64	1.09	1.49	1.10	1.20	1.40	0.82	1.00	1.39	1.03
0.7-10-0.6-40	1.64	1.10	1.49	1.10	1.20	1.40	0.81	0.99	1.42	1.04
0.7-10-0.6-50	1.64	1.10	1.49	1.10	1.19	1.40	0.79	0.97	1.44	1.06
0.7-10-0.6-60	1.64	1.10	1.49	1.10	1.19	1.40	0.79	0.96	1.46	1.07
0.7-10-0.75-30	1.44	1.08	1.47	0.98	1.06	1.41	1.07	1.31	1.08	0.79
0.7-10-0.75-40	1.44	1.08	1.47	0.98	1.06	1.41	1.05	1.28	1.10	0.81
0.7-10-0.75-50	1.44	1.09	1.48	0.98	1.06	1.41	1.03	1.26	1.11	0.82
0.7-10-0.75-60	1.44	1.09	1.48	0.98	1.06	1.41	1.02	1.25	1.13	0.83
0.7-15-0.3-30	1.12	1.10	1.49	0.75	0.82	0.80	0.36	0.44	1.82	1.34
0.7-15-0.3-40	1.12	1.10	1.49	0.75	0.82	0.80	0.35	0.43	1.85	1.36
0.7-15-0.3-50	1.12	1.10	1.50	0.75	0.82	0.80	0.35	0.43	1.88	1.38
0.7-15-0.3-60	1.12	1.10	1.50	0.75	0.82	0.80	0.34	0.42	1.90	1.40
0.7-15-0.45-30	1.10	1.07	1.46	0.75	0.82	1.04	0.58	0.71	1.47	1.08
0.7-15-0.45-40	1.10	1.08	1.46	0.75	0.82	1.04	0.57	0.70	1.49	1.10
0.7-15-0.45-50	1.10	1.08	1.46	0.75	0.82	1.04	0.56	0.69	1.52	1.12
0.7-15-0.45-60	1.10	1.08	1.47	0.75	0.82	1.04	0.55	0.68	1.53	1.13
0.7-15-0.6-30	1.22	1.06	1.44	0.85	0.92	1.33	0.81	0.99	1.34	0.98
0.7-15-0.6-40	1.22	1.06	1.44	0.85	0.92	1.33	0.80	0.98	1.36	1.00
0.7-15-0.6-50	1.22	1.06	1.44	0.85	0.92	1.33	0.79	0.96	1.38	1.01
0.7-15-0.6-60	1.22	1.06	1.44	0.85	0.92	1.33	0.78	0.95	1.40	1.03
0.7-15-0.75-30	1.54	1.04	1.42	1.08	1.18	1.16	1.05	1.29	0.90	0.66
0.7-10-0.75-40	1.55	1.05	1.42	1.09	1.18	1.16	1.04	1.27	0.91	0.67
0.7-15-0.75-50	1.55	1.05	1.42	1.09	1.18	1.16	1.02	1.25	0.93	0.68
0.7-15-0.75-60	1.54	1.05	1.43	1.08	1.18	1.16	1.01	1.24	0.94	0.69
0.7-20-0.3-30	1.12	1.07	1.46	0.77	0.84	0.73	0.36	0.44	1.67	1.23
0.7-20-0.3-40	1.12	1.07	1.46	0.77	0.83	0.62	0.35	0.43	1.45	1.06
0.7-20-0.3-50	1.12	1.07	1.46	0.77	0.83	0.62	0.35	0.42	1.47	1.08
0.7-20-0.3-60	1.12	1.08	1.46	0.77	0.83	0.62	0.34	0.42	1.48	1.09
0.7-20-0.45-30	1.12	1.05	1.42	0.79	0.86	0.85	0.57	0.70	1.21	0.89
0.7-20-0.45-40	1.11	1.05	1.43	0.78	0.85	0.85	0.56	0.69	1.23	0.91
0.7-20-0.45-50	1.11	1.05	1.43	0.78	0.85	0.85	0.56	0.68	1.25	0.92
0.7-20-0.45-60	1.11	1.05	1.43	0.78	0.84	0.85	0.55	0.67	1.26	0.93

Table 3 Continued

Specimen number	Brace					Chord				
	SCF_{FE}	SCF_{P}	SCF_{CID}	SCF_{FE} /SCF_{CID}	SCF_{FE}/ SCF_{P}	SCF_{FE}	SCF_{P}	SCF_{CID}	SCF_{FE}/ SCF_{CID}	SCF_{FE}/ SCF_{P}
0.7-20-0.6-30	1.09	1.03	1.40	0.78	0.85	0.99	0.80	0.99	1.00	0.74
0.7-20-0.6-40	1.09	1.03	1.40	0.78	0.84	0.99	0.79	0.97	1.02	0.75
0.7-20-0.6-50	1.09	1.03	1.41	0.77	0.84	0.99	0.78	0.95	1.04	0.76
0.7-20-0.6-60	1.09	1.04	1.41	0.77	0.84	0.99	0.77	0.94	1.05	0.77
0.7-20-0.75-30	1.09	1.02	1.39	0.79	0.86	1.17	1.05	1.28	0.91	0.67
0.7-20-0.75-40	1.09	1.02	1.39	0.79	0.86	1.17	1.03	1.26	0.93	0.68
0.7-20-0.75-50	1.09	1.02	1.39	0.78	0.86	1.17	1.01	1.24	0.94	0.70
0.7-20-0.75-60	1.08	1.02	1.39	0.78	0.85	1.17	1.00	1.23	0.95	0.70
0.7-25-0.3-30	1.13	1.05	1.43	0.79	0.86	0.45	0.35	0.43	1.04	0.76
0.7-25-0.3-40	1.12	1.05	1.43	0.78	0.85	0.45	0.35	0.43	1.06	0.77
0.7-25-0.3-50	1.12	1.05	1.43	0.78	0.85	0.45	0.34	0.42	1.07	0.79
0.7-25-0.3-60	1.12	1.05	1.43	0.78	0.85	0.45	0.34	0.42	1.08	0.80
0.7-25-0.45-30	1.11	1.03	1.40	0.79	0.86	0.69	0.57	0.70	0.99	0.73
0.7-25-0.45-40	1.12	1.03	1.40	0.80	0.87	0.69	0.56	0.69	1.01	0.74
0.7-25-0.45-50	1.10	1.03	1.40	0.78	0.86	0.69	0.55	0.68	1.02	0.75
0.7-25-0.45-60	1.11	1.03	1.40	0.79	0.86	0.69	0.55	0.67	1.03	0.76
0.7-25-0.6-30	1.10	1.01	1.38	0.80	0.87	0.84	0.80	0.98	0.86	0.63
0.7-25-0.6-40	1.10	1.01	1.38	0.80	0.87	0.84	0.79	0.96	0.87	0.64
0.7-25-0.6-50	1.10	1.02	1.38	0.80	0.86	0.84	0.77	0.95	0.89	0.65
0.7-25-0.6-60	1.10	1.02	1.38	0.80	0.86	0.84	0.77	0.94	0.90	0.66
0.7-25-0.75-30	1.09	1.00	1.36	0.80	0.87	0.97	1.04	1.27	0.76	0.56
0.7-25-0.75-40	1.09	1.00	1.36	0.80	0.87	0.97	1.02	1.25	0.78	0.57
0.7-25-0.75-50	1.10	1.00	1.36	0.81	0.88	0.97	1.01	1.23	0.79	0.58
0.7-25-0.75-60	1.09	1.00	1.36	0.80	0.87	0.97	0.99	1.22	0.80	0.58
Average				0.87	0.96				1.22	0.92
COV				0.025	0.033				0.028	0.039

5. SCF formulae of joints

Based on the results of SCFs determined from the numerous finite element models with different parameters, multiple regression analysis was carried out. Then a series of formulae for SCFs on the brace and chord were proposed for concrete-filled circular chord and square braces K-joints under balanced axial loading.

It should be noted that the design rules given in the current design specifications for welded tubular joints are applicable to the traditional SHS-to-SHS or CHS-to-CHS K-joints only. There is no design rule currently used for the SHS-to-CHS K-joints. Therefore, the design rules for the concrete-filled circular chord and square braces K-joints under axial loading were proposed in this

study based on the design rules for the traditional SHS-to-SHS or CHS-to-CHS K-joints, which depend on the geometric parameters β, 2γ, τ and φ. The proposed design equations were derived from the regression analysis by using SPSS (SPSS 1983, Darren and Mallery 2013).

The proposed equation must correctly reflect the influence of various geometric parameters and concrete strength on the stress concentration factors of concrete-filled circular chord and square braces K-joints. The proposed parametric equation must be easily used in engineering fatigue design. Therefore, based on SCF formulae for square chord and braces K-joints in CIDECT design guide, the general format of the SCF formulae for concrete-filled circular chord and square braces K-joints under balanced axial loading can be expressed as

$$SCF = H(A + B \cdot \beta + C \cdot \beta^2) \cdot (2\gamma)^D \cdot (\tau)^E \cdot (\varphi/60)^F \cdot (\sin(\theta))^G \tag{5}$$

Where the constant A to H will be determined by multiple regression analysis.

According to the results of the multiple regression analysis, the formulae for SCFs of concrete-filled circular chord and square braces K-joints under axial loading are given as follows

Chord member:

$$SCF = 0.6(0.383\beta^2 + 0.983\beta + 0.682) \cdot (2\gamma)^{-0.028} \cdot (\tau)^{1.175} \cdot (\frac{\phi}{60})^{-0.063} \cdot (\sin(\theta))^{0.057} \tag{6}$$

Brace member:

$$SCF = 0.8(-9.680\beta^2 + 11.681\beta - 2.061) \cdot (2\gamma)^{-0.086} \cdot (\tau)^{-0.054} \cdot (\frac{\phi}{60})^{0.006} \cdot (\sin(\theta))^{0.139} \tag{7}$$

The SCFs obtained from the parametric study were compared with the SCFs calculated using the proposed designed equation for concrete-filled circular chord and square braces K-joints. The comparison for all specimens is shown in Table 3. A good agreement was obtained with the average values of FE SCF-to-Proposed SCF ratios (SCF_{FE}/SCF_P) for brace and chord of 0.96, 0.92 and the corresponding COV of 0.033 and 0.039, respectively. Therefore, the proposed design equations were verified to be accurate and reliable for SCFs on braces and chord of concrete-filled circular chord and square braces K-joints under balanced axial loading.

6. Conclusions

A series of experimental and numerical investigations were conducted on concrete-filled circular chord and square braces K-joints to measure stress concentration factors at the chord and braces intersections. The measured SCFs were compared with SCFs for conventional hollow section K-joints under balanced axial loading obtained in the test. Finally, a series of formulae were proposed for SCFs at various hot spot stress locations. The following conclusions were made on the data available.

(1) Maximum stress concentration factor usually occurred at the heel point on brace and chord in both hollow and concrete-filled circular chord and square braces K-joints.
(2) SCFs of the concrete-filled circular chord and square braces K-joints were smaller than the

SCFs of the corresponding hollow circular chord and square brace K-joints.

(3) Effect of concrete strength on SCFs of concrete-filled circular chord and square braces K-joints is very unobvious.

(4) The proposed SCF formulae gave reasonable and safe estimation of SCFs for concrete-filled circular chord and square braces K-joints under balanced axial loading.

Acknowledgments

This research work was supported by the National Natural Science Foundation of China (Nos. 51278209 and 51478047).

References

Ahmadi, H. (2016), "A probability distribution model for SCFs in internally ring-stiffened tubular KT-joints of offshore structures subjected to out-of-plane bending loads", *Ocean Eng*., **116**, 184-199.

Ahmadi, H., Lotfollahi-Yaghin, M.A. and Aminfar, M.H. (2011), "Effect of stress concentration factors on the structural integrity assessment of multi-planar offshore tubular DKT-joints based on the fracture mechanics fatigue reliability approach", *Ocean Eng*., **38**(17-18), 1883-1893.

Ahmadi, H., Lotfollahi-Yaghin, M.A. and Aminfar, M.H. (2012), "The development of fatigue design formulas for the outer brace SCFs in offshore three-planar tubular KT-joints", *Thin-Wall. Struct*., **58**, 67-78.

Ahmadi, H. and Lotfollahi-Yaghin, M.A. (2013), "Effect of SCFs on S-N based fatigue reliability of multi-planar tubular DKT-joints of offshore jacket-type structures", *Ships Offshore Struct*., **8**(1), 55-72.

Ahmadi, H., Ali Lotfollahi-Yaghin, M.A. and Shao, Y.B. (2013), "Chord-side SCF distribution of central brace in internally ring-stiffened tubular KT-joints: A geometrically parametric study", *Thin-Wall. Struct*., **70**, 93-105.

Cao, Y.G., Meng, Z.B., Zhang, S.H. and Tian, H.Q. (2013), "FEM study on the stress concentration factors of K-joints with welding residual stress", *Appl. Ocean Res*., **43**, 195-205.

Chen, J., Chen, J. and Jin, W.L. (2010), "Experiment investigation of stress concentration factor of concrete-filled tubular T-joints", *J. Construct. Steel Res*., **66**(12), 1510-1515.

Cheng, B., Qian, Q. and Zhao, X.L. (2015), "Numerical investigation on stress concentration factors of square bird-beak SHS T-joints subject to axial forces", *Thin-Wall. Struct*., **94**, 435-445.

Chinese Standard (2006), Code for carbon structure steel; GB/T700-2006, China Standards Press, Beijing, China. [In Chinese]

Chinese Standard (2002), Technical specification for welding of steel structure of building; JGJ 81-2002, China Standards Press, Beijing, China. [In Chinese]

Darren, G. and Mallery, P. (2013), SPSS for Windows Step by Step; A Simple Guide and Reference, 11.0 Update.

Diaye, A.N., Hariri, S., Pluvinage, G. and Azari, Z. (2007), "Stress concentration factor analysis for notched welded tubular T-joints", *Int. J. Fatigue*, **29**(8), 1554-1570.

Eurocode 3 (EC3) (2005), Design of Steel Structures—Part 1-8: Design of Joints, European Committee for Standardization, EN 1993-1-8, CEN, Brussels, Belgium.

Gao, F., Shao, Y.B. and Gho, W.M. (2007), "Stress and strain concentration factors of completely overlapped tubular joints under lap brace IPB load", *J. Construct. Steel Res*., **63**(3), 305-316.

Lee, C.K., Chiew, S.P., Lie, S.T. and Nguyen, T.B.N. (2009a), "Fatigue study of partially overlapped circular hollow section K-joints. Part 1: Geometrical models and mesh generation", *Eng. Fract. Mech*., **76**(16), 2445-2463.

Lee, C.K., Chiew, S.P., Lie, S.T. and Nguyen, T.B.N. (2009b), "Fatigue study of partially overlapped circular hollow section K-joints. Part 2: Experimental study and validation of numerical models generation", *Eng. Fract. Mech.*, **76**(15), 2408-2428.

Liu, H.Q., Shao, Y.B., Lu, N. and Wang, Q.L. (2015), "Hysteresis of concrete-filled circular tubular (CFCT) T-joints under axial load", *Steel Compos. Struct., Int. J.*, **18**(3), 739-756.

Pang, N.L., Zhao, X.L., Mashiri, F.R. and Dayawansa, P. (2009), "Full-size testing to determine stress concentration factors of dragline tubular joints", *Eng. Struct.*, **31**(1), 43-56.

Ran, F. and Young, B. (2013), "Stress concentration factors of cold-formed stainless steel tubular X-joints", *J. Construct. Steel Res.*, **91**, 26-41.

Shao, Y.B. (2006), "Analysis of stress intensity factor (SIF) for cracked tubular K-joints subjected to balanced axial load", *Eng. Fail. Anal.*, **13**(1), 44-64.

SPSS Inc. (1983), SPSS/PC: for the IBM PC/XT.

Tong, L.W., Sun, C.Q., Chen, Y.Y., Zhao, X.L., Shen, B. and Liu, C.B. (2008), "Experimental comparison in hot spot stress between CFCHS and CHS K-joints with gap", Tubular Structures XII, (Z.Y. Shen, Y.Y. Chen, X.Z. Zhao Editors), Taylor & Francis, London, UK, pp. 389-395.

Wang, K., Tong, L.W., Zhu, J., Zhao, X.L. and Mashiri, F.R. (2013), "Fatigue behavior of welded T-joints with a CHS brace and CFCHS chord under axial loading in the brace", *J. Bridge Eng.*, **18**(2), 142-152.

Yang, J., Chen, Y. and Hu, K. (2015), "Stress concentration factors of negative large eccentricity tubular N-joints under axial compressive loading in vertical brace", *Thin-Wall. Struct.*, **96**, 359-371.

Zhao, X.L., Herion, S., Packer, J.A., Puthli, R.S., Sedlacek, G., Wardenier, J., Weynand, K., Wingerde, A.M. and Yeomans, N.F. (2001), Design guide for circular and rectangular hollow section welded joints under fatigue loading; CIDECT Design Guide No.8, TUV-Verlag, Cologne, Germany.

CC

Nomenclature

A, B, C, D, E, F, G, H	Coefficients for proposed designed equations
d_0	External diameter of chord
t_0	Thickness of chord
b_1	Side length of brace
t_1	Thickness of brace
θ	Included angle between brace and chord
ψ	Rotation degree of intersection line
β	Ratio of brace side length to chord diameter
2γ	Ratio of chord diameter to chord thickness
τ	Ratio of brace thickness to chord thickness
φ	Strength grade of concrete in chord
CHS	Circular hollow section
SHS	Square hollow section
FE	Finite element
SCF	Stress concentration factor
SNCF	Strain concentration factor
HSSN	Hot spot strain
COV	Coefficient of variation
E	Young's modulus of elasticity
υ	Poisson's ration
SCF*FE*	SCF computed by finite element method
SCF*P*	SCF computed by proposed design equation
SCF*CID*	SCF computed by CIDECT design equation
$\sigma_{\mathrm{h.s}}$	Hot spot stress
σ_{nom}	Nominal stress